Intermolecular Charge-Transfer Luminescence by Self-Assembly of Pyridinium Luminophores in Solutions

Kaspars Leduskrasts and Edgars Suna*[a]

Designing a luminophore for application both in solution and in the solid state is a highly challenging task given the distinct nature of intermolecular interactions in these phases. In this context, we demonstrate that self-assembly of non-emissive charged pyridinium luminophores enables luminescence in solutions through a mechanism that is characteristic for the crystal state. Specifically, protonation of pyridine luminophore subunits in a solution promotes oligomer formation through intermolecular π^{+}-π interactions, leading to an intermolecular charge-transfer type luminescence. The luminescence turn-on by protonation is utilized for a highly efficient solution-state luminescent sensing of hydrogen chloride and sulfonic acids (TfOH, TsOH and MsOH) with detection limits spanning the range from 0.06 to 0.33 ppm. The protonation followed by self-assembly results in a bathochromic shift of the emission from 420 nm to 550 nm.

1. Introduction

A wide range of sensing applications in solutions as well as modern solid state lighting devices is based on light-emitting molecules (luminophores).[1] The vast majority of luminophores feature distinct luminescence mechanisms in solution and in the crystal state.[2a,b] This distinction has been a focus of considerable research efforts during the last two decades.[2] In the crystal state, numerous static intermolecular interactions,[3] such as H-bonds,[4] halogen bonds,[4b,5] π-π interactions,[6] cation-π stacking[7] and electrostatic interactions,[8] greatly impact the luminescence emission pathways, resulting in aggregated luminophore mechanisms (Figure 1). In sharp contrast, the intermolecular interactions in solution are highly dynamic and significantly weakened due to Brownian motion.[9] The weakened intermolecular interactions in solution lead to an emission by isolated luminophore mechanisms. Apparently, the distinct nature of intermolecular interactions in solution and in the crystal state is responsible for the different luminescence mechanisms.

A rare example of a luminescence mechanism that does not differ between the phases is associated with luminophores that exert luminescence through the excited dimer (excimer) mechanism (Figure 1).[10] Excimer emission relies on the formation of a meta-stable excited dimer, which upon emission dissociates into its parent luminophores.[10a,c,e] The excimer emission of purely organic luminophores in the crystal state is promoted by intermolecular π orbital overlap.[10b] A similar π orbital overlap is also achievable in solutions, provided that high enough concentration of the luminophore can be obtained,[11] resulting in excimer-type emission. Unfortunately, the excimer emission cannot be maintained in diluted solutions due to the low collision likelihood between luminophores. Accordingly, achieving intermolecular interactions that are persistent in both the solid and the solution state would open a path to obtain exceptional luminophores with consistent luminescent mechanisms between the phases.

Recently, we have demonstrated that enhanced solid-state emission can be achieved by simple protonation of highly planar conjugated pyridines.[12] The mechanism of the solid-

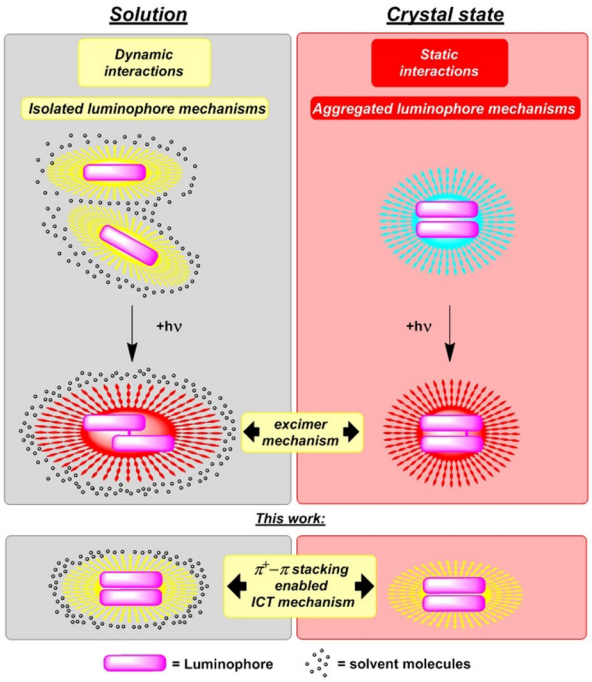

Figure 1. Luminescent properties in solution and in the crystal state.

[a] K. Leduskrasts, Prof. Dr. E. Suna
Latvian Institute of Organic Synthesis
Aizkraukles 21
1006 Riga (Latvia)
E-mail: edgars@osi.lv

Supporting information for this article is available on the WWW under https://doi.org/10.1002/open.202100191

state luminescence involved intermolecular π^+-π and π^+-π^+ interactions.[13] We envisioned that the protonation of planar conjugated pyridine subunits could lead to enhanced emission also in solution, provided that the solvent does not interfere with the key intermolecular π^+-π and π^+-π^+ interactions.[7,14] Herein, we disclose that protonation of pyridine-containing luminophores in diluted solutions of toluene, Et_2O, $CHCl_3$ and EtOAc effects the desired intermolecular π^+-π interactions by self-assembly of the protonated species. The self-assembly in solution leads to emission turn-on through intermolecular charge-transfer (ICT) type luminescence mechanism (Figure 1). Hence, the key intermolecular π^+-π interactions are well-suited for the design of versatile luminogens that exert luminescence both in solution and in the solid state through similar emission mechanisms. The application of the pyridine-containing luminogens for the detection of hydrogen chloride and sulfonic acid in solutions with sensing limits well below 1 ppm is also reported.

2. Results and Discussion

2.1. Spectral Characterization of 3 and 3×HCl in Various Solvents

Pyridine **3** was synthesized from 9-(4-bromophenyl)-9H-carbazole **1** and pyridine-4-boronic acid hydrate **2** (Supporting Information, page S3) by a previously reported protocol.[13a] The UV-Vis absorption and emission spectra of pyridine **3** were recorded in DMF, DMSO, EtOAc, toluene, $CHCl_3$ and Et_2O solutions at room temperature and under ambient atmosphere. The concentration of samples was 10^{-5} M. Pyridine **3** displayed three distinct absorption maxima at 242–262 nm, 290–294 nm and 320–329 nm, respectively, in DMSO, EtOAc, $CHCl_3$ and Et_2O. The absorption maxima could not be measured in the 240–280 nm region for toluene and in the 240–260 nm region for DMF due to the competing absorption by these solvents (Supporting Information, page S5). Additionally, the broad featureless emission maxima of **3** underwent a bathochromic shift from 380 nm in toluene to 443 nm in DMSO (Figure 2A). Next, the UV-Vis absorption and emission spectra of pyridine **3×HCl**[15] were recorded in DMF, DMSO, EtOAc, toluene, $CHCl_3$ and Et_2O solutions. Accordingly, **3×HCl** displayed absorption peaks at 239–263 nm, 278–287 nm and 367–397 nm in DMSO, EtOAc, $CHCl_3$ and Et_2O. The absorption in DMF and toluene could not be measured up to 260 nm and 275 nm, respectively, due to the intrinsic solvent absorption (Supporting Information, page S5). Significant red-shifts were observed for the absorption peaks in all examined solvents upon the protonation of pyridine **3** by hydrogen chloride. For example, a 53 nm bathochromic shift of the absorption peak from 319 nm to 372 nm was measured in Et_2O for **3** in the presence of HCl (Figure 2B).

Notably, lack of emission was observed for pyridine salt **3×HCl** in highly polar solvents such as DMF and DMSO. This observation is in agreement with the previously reported poor luminescence of **3×HCl** in MeCN solution.[12] To gain insight into the origins of the observed emission lack in polar solvents, the luminescence of **3×HCl** in DMSO was compared at room

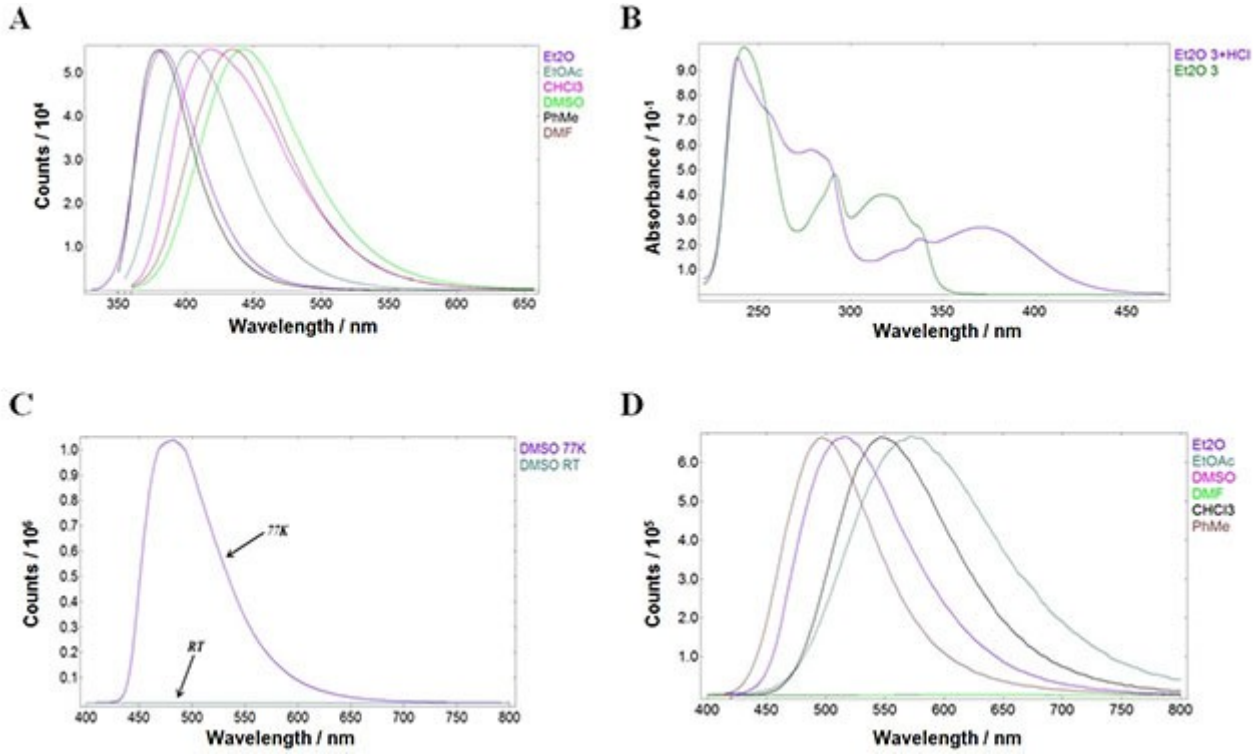

Figure 2. [A] Emission of **3** in various solvents; [B] Absorbtion of **3** and **3×HCl** in Et_2O; [C] Emission of **3×HCl** in DMSO at room temperature and 77 K; [D] Emission of **3×HCl** in various solvents.

temperature to that at 77 K. In sharp contrast to the lack of emission at room temperature, intense luminescence at 483 nm was observed in a frozen DMSO matrix upon cooling **3×HCl** to 77 K (Figure 2C). Importantly, the emission at 77 K displayed a clear afterglow that was observable even with the naked eye. The measured lifetime value for the emission ($\tau = 1.51$ s; Supporting Information, page S6) suggests that long-lived triplet states are responsible for the luminescence at 77 K. The strength of the emission intensity at 77 K is associated with the high triplet state population, apparently because of the highly efficient and rapid intersystem crossing in **3×HCl**. Hence, the lack of emission in DMSO solution at room temperature can be most likely attributed to the non-radiative relaxation of the highly solvated **3×HCl** through molecular motion.

In contrast to the non-luminescent properties of **3×HCl** in highly polar solvents such as DMSO and DMF, an intense emission was observed for **3×HCl** at room temperature in less polar solvents. Specifically, an intense, broad and featureless emission with a strong solvatochromic effect was observed in toluene (emission maximum at 497 nm), Et_2O (at 516 nm), $CHCl_3$ (at 548 nm) and EtOAc (at 574 nm; Figure 2D). The observed distinct luminescence behavior of **3×HCl** in high- and low-polarity solvents could be attributed to their different solvating ability. Thus, the polar solvents (DMSO, DMF) of high solvating ability stabilize monomers of **3×HCl**. The lack of the emission for **3×HCl** in DMSO and DMF at room temperature suggests that monomeric species of **3×HCl** are non-emissive. In contrast, solvents of a lesser solvating ability, such as EtOAc, $CHCl_3$, Et_2O and toluene, should favor the formation of intermolecular interactions between **3×HCl**. We hypothesized that the observed room temperature emission of **3×HCl** in EtOAc, $CHCl_3$, Et_2O and toluene may be attributed to the formation of aggregates. Dynamic light scattering (DLS) measurements were employed to verify whether aggregates are responsible for the observed emission. However, DLS measurements did not support the presence of higher aggregates in the luminescent solutions of **3×HCl**. Since smaller oligomers such as dimers or trimers fall below the detection limits of DLS, additional experiments were required to verify the possible involvement of small oligomers in the emission of **3×HCl**.

2.2. T_1 NMR Experiments

Strong evidence supporting the presence of small oligomers (dimers or trimers) in $CHCl_3$ solutions of **3×HCl** was obtained by longitudinal relaxation time (T_1) nuclear magnetic resonance (NMR) experiments. In the experiment, a decrease in spin lattice relaxation time (T_1) is observed for those molecules that feature intermolecular interactions, because the resulting aggregated species possess larger size and stronger inertia moments.[9] Accordingly, the spin lattice relaxation time (T_1) was measured for **3×HCl** in DMSO-d_6 and $CDCl_3$ solutions (Supporting Information, page S6). For a better representation of changes in T_1 relaxation times in the two solvents, the measured T_1 values in DMSO-d_6 were divided by the respective T_1 values in $CDCl_3$ for each of positions 1–8 in the luminophore molecule **3×HCl** (for the numbering, see Figure 3A). Notably, a significant drop (from 4 to 39 times) of T_1 values was observed for protons in positions 1–4 in $CDCl_3$ solution as compared to those in DMSO-d_6 as the solvent. In contrast, smaller (less than 2 times) differences in T_1 values in the two solvents were measured for

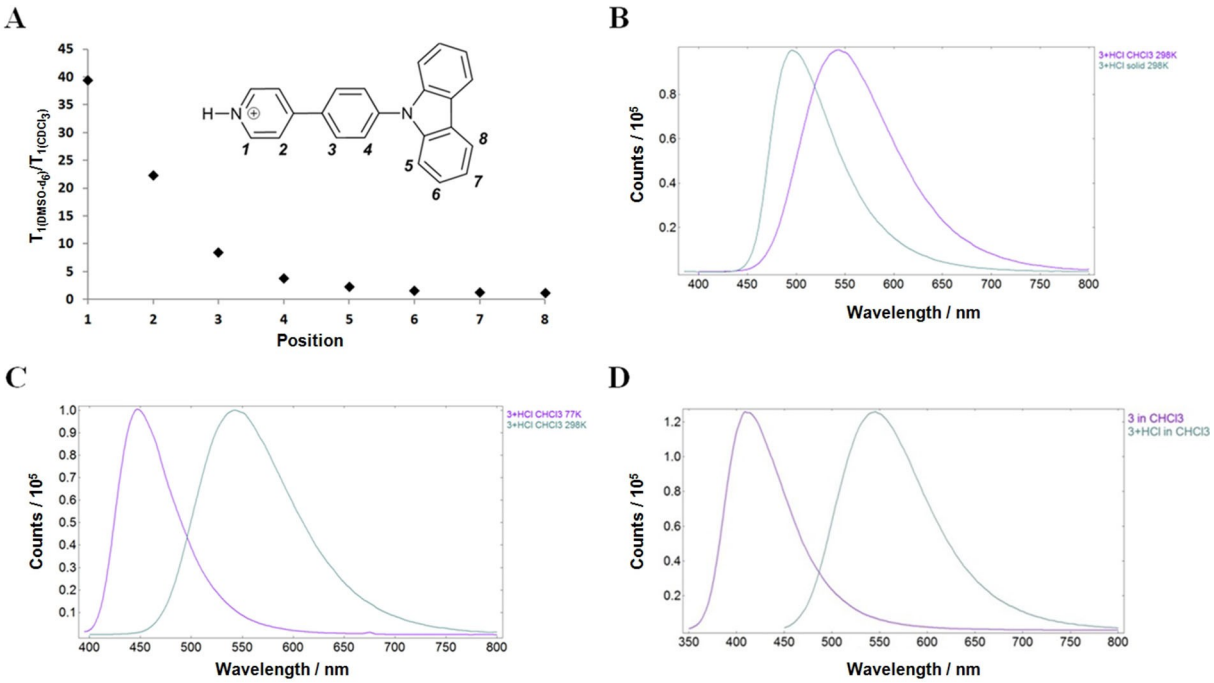

Figure 3. [A] Relative change of T_1 relaxation times at positions 1–8 of **3×HCl** in DMSO-d_6 and $CDCl_3$ solutions; [B] Emission of **3×HCl** in solid state and solution; [C] Emission of **3×HCl** in $CHCl_3$ at 298 K and 77 K; [D] Emission spectra of **3** in $CHCl_3$ before (left), after (right) addition of HCl;

positions 5–8. These results provide strong evidence for the presence of intermolecular interactions between protonated pyridine species **3×HCl** in $CDCl_3$ solution. Furthermore, only the pyridinium subunit and the phenylene linker appear subjected to these intermolecular interactions. In contrast, the carbazole moiety is not involved as evidenced by the NMR experiments. Hence, the spin lattice relaxation time measurements suggest that the observed luminescence in $CHCl_3$, EtOAc, Et_2O and toluene is a result of intermolecular pyridinium-pyridinium π^+-π interactions of protonated luminogen **3×HCl** in solution.[12,13]

2.3. Charge-Transfer Emission

Additional indirect support for the formation of intermolecular pyridinium-pyridinium π^+-π interactions in $CHCl_3$ solution of protonated luminogen **3×HCl** was provided by the comparison of its luminescent properties in the solid state with those in the solution. It has been demonstrated earlier that the observed broad featureless emission of pyridinium salts such as **3×HCl** in the solid state is indicative of intermolecular π^+-π charge-transfer (ICT) mechanism for the luminescence.[12,13,16] Importantly, featureless emission for **3×HCl** was also observed in $CHCl_3$ solution. Furthermore, a red-shift of emission maximum from 496 nm in the solid state to 548 nm in the $CHCl_3$ solution was measured (Figure 3B). In the meantime, cooling the $CHCl_3$ solution of **3×HCl** from 293 K to 77 K resulted in a blue-shift from 548 nm to 448 nm, respectively (Figure 3C). The apparent dependence of the luminescence maximum on the rigidity of molecular environment (rigidochromism) points to the ICT mechanism for **3×HCl** due to a polarization flip between ground and excited states.[17] The observed blue-shift for **3×HCl** is associated with the reduced degree of stabilization of the luminophore excited state by solvent molecules in a frozen matrix at 77 K. An additional evidence for the CT emission for **3×HCl** was also obtained from the observed strong solvatochromic effect between PhMe, $CHCl_3$, EtOAc and Et_2O (Figure 2D).[18] Finally, the observed emission for **3×HCl** in weakly coordinating solvents at concentrations as low as 10^{-7} M helped to rule out the excimer-type emission that usually requires much higher concentrations, typically around 10^{-3} M.[11b] Hence, the luminescence data provide strong support for the ICT emission mechanism enabled by π^+-π interactions between the protonated species of **3×HCl** in relatively non-polar solvents such as $CHCl_3$, EtOAc, Et_2O and PhMe.

2.4. Sensing of HCl

The observed bathochromic shift of the emission maximum from 418 nm for **3** to 548 nm for **3×HCl** (Figure 3D) in the presence of hydrogen chloride is a result of a two-step process: 1) protonation of the pyridine luminophore resulting in a non-emissive monomer, and 2) the formation of oligomers through π^+-π interactions, which leads to the intermolecular CT emission. We realized that such an emission mechanism is well-suited for the design of luminescent sensors. The luminescence response and emission properties of **3** in $CHCl_3$ were examined in the presence of HCl vapours (see Figure 4 and Videos S1 and S2 in the Supporting Information). Gratifyingly, a distinct emission change from colourless to pale green was observed under ambient light after the $CHCl_3$ solution of **3** was subjected to hydrogen chloride vapours. The colour change was more pronounced when observed under UV light (365 nm). Accordingly, the $CHCl_3$ solution of **3** emits violet light, and a change to green emission occurred upon exposure to HCl vapours (Figure 4; see also Supporting Information, page S17). A similar sensory response was observed for MsOH, TsOH, TfOH and TFA by pyridine-derived luminogen **3** (Supporting Information, pages S7–S9). Hence, the solution of **3** demonstrates a response to the presence of various strong acids. The sensory response time towards acids is as fast as the diffusion of the acid within the solution (Video 2 in Supporting Information).

2.5. Determining the Limit of Detection (LoD)

A statistical approach was used at the 95% confidence level to determine the limit of detection (LoD) for HCl, MsOH, TsOH, TfOH and TFA by pyridine-derived luminogen **3**. Assuming that the Gaussian distribution holds true,[19] the LoD was determined from the linear range of the calibration plot (Eq. (1); see also Supporting Information pages S9–S16).

$$LoD = \frac{m_{blank} + 3.29 \times \sigma_{(blank)}}{b} \quad (1)$$

where $m_{(blank)}$ = the mean value of blank measurements; $\sigma_{(blank)}$ = standard deviation of blank measurements; b = the slope of the linear equation.

The linear range of the calibration plot was obtained by conducting additional measurements for each of the acids (Supporting Information, pages S10–S15). The obtained $\sigma_{(blank)}$ was in the range from 23–33 counts per second (Supporting Information, pages S9–S10). Accordingly, the calculated LoD for the tested acids decrease in the following order (Supporting Information, pages S15–S16): MsOH (0.06 ppm) > TfOH (0.13 ppm) > TsOH (0.19 ppm) > HCl (0.33 ppm) > TFA (8.1 ppm)

The determined detection limits for sulfonic acids (TfOH, TsOH and MsOH) were similar to that for hydrochloric acid,

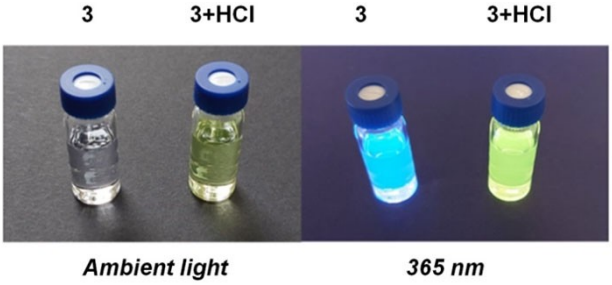

Figure 4. $CHCl_3$ solution of **3** before and after exposure to HCl vapours at ambient light and at 365 nm excitation.

falling within the range from 0.06 ppm to 0.33 ppm. However, luminophore **3** was less sensitive (by two orders of magnitude) towards TFA (8.1 ppm). Notably, the detection limit for acids correlated well with their equilibrium acidity values. Thus, luminophore **3** demonstrated highest sensitivity towards strong acids such as hydrogen chloride ($pK_{a,MeCN} = 10.3$),[20] MsOH ($pK_{a,MeCN} = 9.97$),[20] TsOH ($pK_{a,MeCN} = 8.45$)[21] and TfOH ($pK_{a,\ MeCN} = 2.6$).[21] In contrast, **3** featured reduced sensitivity towards TFA ($pK_{a,MeCN} = 12.65$),[21] which is the weakest among all tested acids. The observed correlation between the equilibrium acidity values and the LoD is consistent with the proposed sensing mechanism that relies on the protonation of the pyridine subunit in luminophore **3**, leading to intermolecular pyridinium-pyridinium π^+-π interactions of **3**×**HCl**. Notably, the pyridine **3**-derived hydrogen chloride sensor features considerably higher (more than two orders of magnitude) sensitivity when compared to that of most potent Schiff-base sensors (54 ppm).[22]

3. Conclusion

Intermolecular charge transfer type (ICT) emission in solution can be achieved by self-assembly of individually non-emissive pyridinium-containing luminophores. Spin-lattice relaxation (T_1) time NMR experiments in $CDCl_3$ solution provided strong evidence for the self-assembly and oligomer formation through intermolecular π^+-π interactions. The proposed ICT mechanism for the luminescence is consistent with the non-emissive nature of the pyridinium luminophore in polar solvents such as DMSO and DMF, where the highly solvated monomeric luminophore undergoes non-radiative relaxation through molecular motions. Additional support for the ICT mechanism was also obtained from the observed solvatochromism and emission dependence on the rigidity of molecular environment. Importantly, the intermolecular interactions of non-excited pyridine luminophores that are observable by NMR methods together with the emission in highly diluted (as low as 10^{-7} M) solutions speak against the excimer emission mechanism. The ICT luminescence in solutions allows for the use of easy-to-synthesise, robust and inexpensive planar pyridine-derived luminophore 3 as a sensor for the detection of hydrogen chloride as well as other relatively strong acids such as sulfonic acids (TfOH, TsOH and MsOH) with sensing limits (LoD) spanning the range from 0.06 ppm to 0.33 ppm. Less acidic carboxylic acids such as TFA could be also determined, however with reduced sensitivity (8.1 ppm LoD). The exposure of solutions of luminophore 3 in EtOAc, toluene, $CHCl_3$ or Et_2O to HCl gas and organic acids brings about a rapid emission increase at 550 nm. The importance of the pyridinium salt formation for the luminescent response is corroborated by the observed correlation between LoD and the thermodynamic acidity (pK_a) values for various acids. Overall, the use of intermolecular π^+-π CT type interactions in solutions opens ample opportunities for the rational design of luminescent materials and sensors.

Acknowledgements

This work was funded by ERDF (project No. 1.1.1.1/18/A/063 "Next Generation Aggregation Induced Emission Luminogens for Artificial Lighting Sources"). We thank Prof. Dr. K. Jaudzems for assistance with NMR experiments.

Conflict of Interest

The authors declare no conflict of interest.

Keywords: aggregation-induced emission · intermolecular interactions · luminescent property transfer · self-assembly · sensors

[1] a) Y. Zhou, J. Yoon, *Chem. Soc. Rev.* **2012**, *41*, 52; b) Y. Liu, C. Li, Z. Ren, S. Yan, M. R. Bryce, *Nat. Rev. Mater.* **2018**, *3*, 18020; c) S. Kanagaraj, A. Puthanveedu, Y. Choe, *Adv. Funct. Mater.* **2019**, *30*, 1907126; d) S. Chowdhury, B. Rooj, A. Dutta, U. Mandal, *J. Fluoresc.* **2018**, *28*, 999.
[2] For representative reviews, see: a) S. Mukherjee, P. Thilagar, *Chem. Commun.* **2015**, *51*, 10988; b) Kenry, C. Chen, B. Liu, *Nat. Commun.* **2019**, *10*, 1; c) J. Mei, N. L. Leung, R. T. Kwok, J. W. Lam, B. Z. Tang, *Chem. Rev.* **2015**, *115*, 11718; d) Z. Zhao, H. Zhang, J. W. Lam, B. Z. Tang, *Angew. Chem. Int. Ed.* **2020**, *59*, 9888; e) J. Yang, M. Fang, Z. Li, *InfoMat* **2020**, *2*, 791; f) W. Jia, Q. Wang, H. Shi, Z. An, W. Huang, *Chem. Eur. J.* **2020**, *26*, 4437; g) A. D. Nidhankar, Goudappagouda, V. C. Wakchaure, S. S. Babu, *Chem. Sci.* **2021**, *12*, 4216; h) J. Mei, Y. Hong, J. W. Lam, A. Qin, Y. Tang, B. Z. Tang, *Adv. Mater.* **2014**, *26*, 5429.
[3] J.-P. Zhang, P.-Q. Liao, H.-L. Zhou, R.-B. Lin, X.-M. Chen, *Chem. Soc. Rev.* **2014**, *43*, 5789.
[4] a) T. Zhang, H. Gao, A. Lv, Z. Wang, Y. Gong, D. Ding, H. Ma, Y. Zhang, W. Z. Yuan, *J. Mater. Chem. C* **2019**, *7*, 9095; b) L. Xiao, H. Fu, *Chem. Eur. J.* **2018**, *25*, 714.
[5] W. Wang, Y. Zhang, W. J. Jin, *Coord. Chem. Rev.* **2020**, *404*, 213107.
[6] a) A. S. Klymchenko, *Acc. Chem. Res.* **2017**, *50*, 366; b) S. A. Jenekhe, J. A. Osaheni, *Science* **1994**, *265*, 765.
[7] S. Yamada, *Coord. Chem. Rev.* **2020**, *415*, 213301.
[8] a) B. A. Naqvi, M. Schmid, E. Crovini, P. Sahay, T. Naujoks, F. Rodella, Z. Zhang, P. Strohriegl, S. Bräse, E. Zysman-Colman, W. Brütting, *Front. Chem.* **2020**, *8*, 750; b) J. Wang, X. Gu, P. Zhang, X. Huang, X. Zheng, M. Chen, H. Feng, R. T. Kwok, J. W. Lam, B. Z. Tang, *J. Am. Chem. Soc.* **2017**, *139*, 16974.
[9] V. I. Bakhmutov, *Practical NMR relaxation for chemists*, Wiley, Chichester, West Sussex, England, **2004**.
[10] a) V. Tkachenko, *Optical Spectroscopy: Methods and Instrumentations*, Elsevier, **2006**; b) Y. Ge, Y. Wen, H. Liu, T. Lu, Y. Yu, X. Zhang, B. Li, S.-T. Zhang, W. Li, B. Yang, *J. Mater. Chem. C* **2020**, *8*, 11830; c) J. B. Birks, *Rep. Prog. Phys.* **1975**, *38*, 903; d) G. W. Gokel, L. J. Barbour, *Comprehensive Supramolecular Chemistry II*, Elsevier, Amsterdam, Netherlands, **2017**; e) J. C. Lindon, G. E. Tranter, D. W. Koppenaal, *Encyclopedia of Spectroscopy and Spectrometry*, Academic Press, Amsterdam, **2017**.
[11] a) R. Katoh, K. Suzuki, A. Furube, M. Kotani, K. Tokumaru, *J. Phys. Chem. C* **2009**, *113*, 2961; b) P. C. Johnson, H. W. Offen, *J. Chem. Phys.* **1973**, *59*, 801.
[12] K. Leduskrasts, E. Suna, *RSC Adv.* **2020**, *10*, 38107.
[13] a) K. Leduskrasts, A. Kinens, E. Suna, *Chem. Commun.* **2019**, *55*, 12663; b) K. Leduskrasts, E. Suna, *RSC Adv.* **2019**, *9*, 460.
[14] a) I. Richter, J. Minari, P. Axe, J. P. Lowe, T. D. James, K. Sakurai, S. D. Bull, J. S. Fossey, *Chem. Commun.* **2008**, 1082; b) W. Chen, S. A. Elfeky, Y. Nonne, L. Male, K. Ahmed, C. Amiable, P. Axe, S. Yamada, T. D. James, S. D. Bull, J. S. Fossey, *Chem. Commun.* **2011**, *47*, 253; c) Y.-J. Huang, Y.-B. Jiang, S. D. Bull, J. S. Fossey, T. D. James, *Chem. Commun.* **2010**, *46*, 8180; d) Excimer emission mechanism through intermolecular π^+-π interactions has also been proposed in certain pyridinium salts in the solid state: X. Cui, Y. Hao, W. Guan, L. Liu, W. Shi, C. Lu, *Adv. Opt. Mater.* **2020**, *8*, 2000125.
[15] 50 equiv. of HCl were added to the solution of **3** in various solvents.

[16] a) S. Sasaki, G. P. Drummen, G.-I. Konishi, *J. Mater. Chem. C* **2016**, *4*, 2731; b) F. B. Dias, S. Pollock, G. Hedley, L.-O. Pålsson, A. Monkman, I. I. Perepichka, I. F. Perepichka, M. Tavasli, M. R. Bryce, *J. Phys. Chem. B* **2006**, *110*, 19329; c) A. Petrozza, F. Laquai, I. A. Howard, J.-S. Kim, R. H. Friend, *Phys. Rev. B* **2010**, *81*, 205421.
[17] A. J. Lees, *Comments Inorg. Chem.* **1995**, *17*, 319.
[18] a) B. Carlotti, R. Flamini, I. Kikaš, U. Mazzucato, A. Spalletti, *Chem. Phys.* **2012**, *407*, 9; b) V. Martínez-Martínez, J. Lim, J. Bañuelos, I. López-Arbeloa, O. Š. Miljanić, *Phys. Chem. Chem. Phys.* **2013**, *15*, 18023; c) E. Sucre-Rosales, R. Fernández-Terán, N. Urdaneta, F. E. Hernández, L. Echevarria, *Chem. Phys.* **2020**, *537*, 110854.
[19] D. A. Armbruster, T. Pry, *Clin. Biochem. Rev.* **2008**, *29*, (Suppl 1) S49.
[20] A. Kütt, T. Rodima, J. Saame, E. Raamat, V. Mäemets, I. Kaljurand, I. A. Koppel, R. Y. Garlyauskayte, Y. L. Yagupolskii, L. M. Yagupolskii, E. Bernhardt, H. Willner, I. Leito, *J. Org. Chem.* **2011**, *76*, 391.
[21] F. Eckert, I. Leito, I. Kaljurand, A. Kütt, A. Klamt, M. Diedenhofen, *J. Comput. Chem.* **2009**, *30*, 799.
[22] X.-C. Li, C.-Y. Wang, Y. Wan, W.-Y. Lai, L. Zhao, M.-F. Yin, W. Huang, *Chem. Commun.* **2016**, *52*, 2748.

Manuscript received: August 5, 2021
Revised manuscript received: October 5, 2021